

# Optical absorption in $ZrO_{2-x}$ -C nanocomposite films on polymer substrates : application of an effective medium theory

P. Cheyssac<sup>1</sup>, N. Laidani<sup>2\*</sup>, M. Anderle<sup>2</sup>,

<sup>1</sup> Laboratoire de Physique de la Matière Condensée, UMR 6622 CNRS, Faculté des Sciences, Parc Valrose, 06108 Nice Cedex 2 (France);

<sup>2</sup> Fondazione Bruno Kessler – Istituto per la Ricerca Scientifica e Tecnologica, Via Sommarive 18, 38050 Povo (Trento), Italy.

**PACS:** 78.20.-e, 78.20.Ci, 78.30.Ly, 78.66.Sq

Films consisting of amorphous carbon dispersed in tetragonal nanocrystalline zirconia were characterized for their optical properties by reflectance measurements. The optical constants of each component of the composite have been extracted; the experimental reflectance spectra have been fitted to Maxwell-Garnett effective medium theory, leading to the effective dielectric constants of the film. Absorption is characterized by the band gap, the energy and lifetime of the optical transition of the absorbing carbon phase. These parameters are deduced from the imaginary part of the dielectric function using Tauc-Lorentz model (TL) and from the extinction coefficient using Forouhi-Bloomer model (FB) in which an energy dependence of the matrix element of the transition has been introduced. Furthermore, the energies of the peak transition and the maximum of the extinction coefficient are so similar that they prove the self-consistency of the modified-FB model applied to the amorphous carbon phase of the composite films.

## 1- Introduction

Transparent conductive oxides have received considerable attention since the increasing demand for materials of low electrical resistance and high transparency in the UV-visible-near IR range. Few studies concern the potentiality of  $ZrO_2$  - based materials as conductor oxydes; they deal essentially with doping [1-3]. On another hand, carbon has been widely used as additive in insulator matrices in order to increase the conductivity of the composite via percolation or percolation-tunneling mechanisms [4-7]. In this work, the optical properties of composite films of  $ZrO_{2-x}$  and carbon deposited onto polycarbonate substrates, have been determined by means of reflectance measurements over the visible range. Parametrization models for optical absorption in semi-conductors, such as Tauc-Lorentz's (TL) [8] and Forouhi-Bloomer's (FB) [9] were applied to the optical constants of the carbon phase. Validity of the models is checked, introducing a figure-of-merit based on equalities of peak transition and maximum absorption energies derived from the models. The electron transitions in the transparent matrix are described by the loss features which accompany the core level spectra measured by x-ray photoelectron spectroscopy (XPS).

## 2- Experimental

Zirconia-carbon films are deposited on polycarbonate (PC) substrates by a r. f. sputtering of two separated targets: monoclinic zirconia and graphite, with respectively 300 W and 100 W applied

---

\* Corresponding author: E-mail: [laidani@itc.it](mailto:laidani@itc.it), Phone: +39-0461 314453, Fax: +39-0461 810851

power chamber and a 0.5 Pa argon pressure. The samples are mounted on a rotating holder, without any external heating.

The film thickness is measured with a stylus Dektak profilometer.

XPS is performed with a Scienta ESCA 200 spectrometer, with monochromatized AlK $\alpha$  ray. C1s, Zr3d and O1s core level peaks and the valence band are measured on the film surface. A Shirley background subtraction is applied to the spectra. Scienta sensitivity factors is used for element quantification. The electron energy losses (EEL) associated with the excitation of the Zr3d and O1s core levels have been also studied in order to determine the electronic properties of zirconia : band gap, optical transitions and plasmons of zirconia.

Optical reflectance at normal incidence is measured with a Jasco V-550 spectrophotometer, provided with a Czerny-Turner single monochromator and a photomultiplier, in the 400-800 nm range.

### 3- Results and discussion

#### 3.1- Description of the film composition and fill factor determination:

Earlier XPS and x-ray diffraction [10] analyses of films deposited with similar plasma conditions as the present ones have led to chemical and structural characterization. The C1s spectrum lineshape and energy (284.5 eV) corresponded to amorphous carbon, essentially in sp<sup>2</sup> hybridisation state (i. e. graphite-like). X-ray diffraction patterns were typical of a tetragonal phase with grain size 46 nm. Current films contain 10 at.% of carbon and a O/Zr atomic ratio of 1.44, so they will be referred to as ZrO<sub>2-x</sub>-C.

The mass density of zirconia matrix and carbon phase were taken respectively as 5.76 g/cm<sup>3</sup> [11] and 1.9 g/cm<sup>3</sup> [12]. The volume fraction or filling factor of carbon in the composite structure is then deduced to be 0.09.

#### 3.2- Optical transitions of zirconia matrix from EEL spectra:

The upper valence band (VB) of zirconia consists of filled O 2p states. The Zr<sup>4+</sup> ion has empty 4d states and, higher up, empty 5s states. The lower VB consists of Zr 4p states and in between lies O 2s ones. Fig. 1(a) shows a typical VB spectrum of our films. An electric charge appears on the surface of the film during measurements and causes a shift of the spectrum towards higher binding energy. Taking the Fermi level as origin, a correction was introduced with reference to Zr 3d<sub>5/2</sub> binding energy set at 181.8 eV [10]. Extrapolating linearly to zero the highest part of the spectrum due to the O2p band yields a VB maximum at 2.3 eV.

Zirconia is a material with a wide band gap located in the UV. The EEL occur in inelastic processes of band-to-band excitations and plasmons; X-rays measurements of EEL lead to the gap of such dielectrics. In zirconia, some interband transitions with single electron occur at energies lower than collective ones (plasma oscillations). Bulk plasmon excitation occurs at ~26 eV [13] although they can also be observed at ~14 eV, [14, 15]. Loss features due to interband transitions below the plasmon energy are mainly due to: i) O 2p – Zr 4d, at 6-8 eV according to [16], and at 7-11 eV [14]; ii) O 2p – Zr 5s given at 9.5 eV [13], and to: iii) O 2p – O 3s at 13.5 eV [13]. These transitions are visible in the EEL spectrum associated with Zr 3d, as shown in Fig. 1(b). After background subtraction, the curve deconvolution gives three peaks: A at 9.3 eV, B at 12.9 eV and C at 15.2 eV from the Zr 3d<sub>5/2</sub> elastic peak. Peak A can be attributed to one of the two interband transitions that involve Zr 4d or 5s final states. C may be due to bulk plasmon excitation while B may be assigned at either an O 2p – O 3s transition or a surface plasmon.

The band gap E<sub>g</sub> is the onset of the O2p - Zr4d transition, i.e. the onset of the lowest excitation in an EEL spectrum. E<sub>g</sub> is estimated by a linear extrapolation to a minimum of intensity of the low energy portion of the first loss feature in the EEL spectrum associated with Zr 3d and O 1s core level lines.

More accurately, it was also determined as the zero energy in the derivative spectra. This is shown in Fig. 2 (a-b) where both spectra are displayed.

One obtains  $E_g$  as  $5.30 \pm 0.3$  eV and  $4.97 \pm 0.3$  eV on the O1s and Zr3d loss spectrum respectively, showing a good consistency between each other. They are comparable to the direct band-gap energy of ZrO<sub>2</sub> [15 – 17].

These results confirm that for our films, although the zirconia phase is under-stoichiometric, it remains transparent in the visible. This is taken into account for the interpretation of the reflectance measurements leading to the optical constants of the composite film as discussed in the following section.

### 3.3- Optical constants calculations from a Maxwell-Garnett model of reflectance spectra

Optical measurements were made on a 398 nm thick ZrO<sub>2-x</sub>-C film deposited on a 1.02 mm thick PC substrate, a structure sketched in Fig. 3(a).

Both substrate and film are transparent in the visible range of wavelengths  $\lambda$ . During reflectance measurements, the response of the spectrophotometer to energy reflected by the rear face of the samples has been minimized with a light absorbent deposited onto it.

Fig. 3(b) gives the experimental and calculated reflectance spectra of the composite film deposited onto PC as well as that of PC. The film spectrum shows the characteristic interference pattern of transparent layered structures, as it will be demonstrated below.

Polycarbonate exhibits a rather flat spectrum except in a close vicinity of 400 nm.

The real part  $v_p$  of its index  $n_p = v_p + i \kappa_p$  is given by

$$v_p = a + b\lambda + \frac{c}{\lambda^2} \quad (1)$$

in which  $a = 1.532$ ,  $b = 2.585 \cdot 10^{-4} \text{ nm}^{-1}$  and  $c = 26.750 \cdot 10^3 \text{ nm}^2$ . This flat spectrum is in good agreement with already published data [18].

However, one cannot be sure that the film deposition process leaves the PC index identical to that of a bare and non-treated substrate. Actually, this has been taken into account introducing an imaginary part

$$\kappa_p = a' + b'\lambda^2 + \frac{c'}{\lambda^2} \quad (2)$$

where  $a' = 9.37 \cdot 10^{-3}$ ,  $b' = -710^{-9} \text{ nm}^{-2}$  and  $c' = 847.88 \text{ nm}^2$

The amplitude of the electric field reflected by the sample is described according to the classical principles of propagation of electromagnetic waves, discussed by Born and Wolf [19]: namely we consider a plane and parallel layer of composite film deposited on a semi-infinite substrate of polycarbonate whose indices are given above. Since the rear face of polycarbonate is coated and absorbing, no wave is back reflected; the combination of interfaces becomes rather straightforward although complex values of indices have to be handled with care.

Let  $n_i$  be the index of the  $i$ -th layer. The reflectance coefficients  $\rho_{ij}$  of the various interfaces are

$$\rho_{ij} = \frac{n_i - n_j}{n_i + n_j} \quad (3)$$

with  $\rho_{12}$  for the vacuum-film interface, and  $\rho_{23}$  for film-polycarbonate interface. Then, the theoretical expression of Fresnel reflectance is  $R_{Fresnel} = \rho\rho^*$  with

$$\rho = \frac{\rho_{12} + \rho_{23} e^{2ik_2 d_2}}{1 + \rho_{12} \rho_{23} e^{2ik_2 d_2}} \quad (4)$$

where  $k_i$  is the wave vector and  $d_2$  the thickness of the composite layer [20].

The effective dielectric constant of the composite film,  $\langle \epsilon \rangle$ , can be found applying Maxwell-Garnett equation [21]

$$\langle \varepsilon \rangle = \varepsilon_m \frac{1 - q + 3 \varepsilon A}{1 - q + 3 \varepsilon_m A} \quad (5)$$

where  $q$  is the volume fraction occupied by carbon and  $\varepsilon$  its dielectric constant.  $\varepsilon_m$  stands for the matrix constant i.e. zirconia, and  $A = q / \varepsilon + 2 \varepsilon_m$ .

The effective refractive index of the film  $\langle n \rangle = \sqrt{\langle \varepsilon \rangle}$  is the unknown parameter to be determined by fitting the experimental reflectance spectrum. The fit is based on calculating  $R_{Fresnel}$  as above, by (i) introducing  $\varepsilon_p$ ,  $\varepsilon$  and  $\varepsilon_m$  for polycarbonate, C and zirconia phases of the film respectively, (ii) calculating  $\langle \varepsilon \rangle$  using Maxwell-Garnett model and (iii) applying equation (4) to calculate the reflectance coefficient and its conjugate, both entering in the reflectance determination.

Inputs in the calculations are indices of polycarbonate given above, optical indices  $n = \nu + i \kappa$  of carbon and  $n_m = \nu_m + i \kappa_m$  of zirconia, and the measured film thickness  $d_2 = 398$  nm.

As starting point of the calculations, the indices of diamond and zirconia replace those of the carbon and zirconia phases of the composite film.

The real part  $\nu$  of the index is described by a dispersion relation such as

$$\nu^2 = a + \frac{b \lambda^2}{\lambda^2 - d} + \frac{c \lambda^2}{\lambda^2 - e} \quad (6)$$

in which the coefficients are given below for  $\lambda$  expressed in nm [22], corresponding units being not written.

For diamond :  $a = 2.309828$ ,  $b = 3.356515$ ,  $c = 17300$ ,  $d = 3.356515$  and  $e = 2.5 \cdot 10^9$ .

For zirconia:  $a = 2.051223$ ,  $b = 2.414018$ ,  $c = 26482.75$ ,  $d = 11.25$  and  $e = 7 \times 10^8$

Moreover, evaporated or sputtered carbons are known to be absorbing; such absorption has been taken into account introducing an imaginary part in its index

$$\kappa = a'_c + \frac{b'_c}{\lambda} \quad (7)$$

where  $a'_c = -0.169$  and  $b'_c = 143.8$ . Let us remind that zirconia remains without absorption.

The calculated reflectance is fitted to the experimental spectrum by a least square procedure. As a result, the best fit is obtained with the following coefficients: the calculated thickness  $d_2 = 405$  nm, is very close to the measured one; for carbon,  $b = 2.084$  and  $c = 9400$  alone are modified. For zirconia,  $a = 1.920$ ,  $b = 2.360$ ,  $c = 20982$ ,  $d = 11.25$  and  $e = 8 \times 10^8$ .

As it can be seen in Fig.3 (b), the fit can be considered as satisfying over most of the energy range.

The optical properties of carbon in the visible range are then described by the real and imaginary parts of either its index  $n = \nu + i \kappa$  or its dielectric function  $\varepsilon = \varepsilon_1 + i \varepsilon_2$  which realize the best fit to the experimental reflectance spectrum. The same can be said for zirconia:  $n_m = \nu_m + i \kappa_m$  and  $\varepsilon_m = \varepsilon_{m1} + i \varepsilon_{m2}$ .

The obtained optical constants are displayed in Fig. 4 (a-b). They were used to study the absorption properties, i.e. electronic transition parameters of the carbon phase of the film.

#### 3.4- Transition lifetime $\tau$ , energy gap $E_g$ and peak transition energy $E_0$ deduced from optical measurements

Several models have been developed and describe the electronic transition parameters such as the band gap, the peak transition energy  $E_0$  and the transition lifetime. Models from Tauc-Lorentz (TL) [8] and Forouhi-Bloomer (FB) [9] are widely used. In this work, they have been applied to the optical constants of the carbon phase of the composite film. In Tauc-Lorentz model  $\varepsilon_2(E)$  is given as

$$\varepsilon_2(E) = \frac{1}{E} \frac{AE_0 \Gamma (E - E_g)^2}{[(E^2 - E_0^2)^2 + \Gamma^2 E^2]} \quad \text{for } E > E_g \quad (8)$$

and  $\varepsilon_2(E) = 0$  for  $E \leq E_g$ . (9)

where  $A$  is the amplitude factor and  $\Gamma$  the broadening parameter.

In FB formalism as in TL's,  $\tau$ ,  $E_g$  and  $E_0$  can be derived. This is achieved by fitting  $\kappa(E)$  as follows

$$\kappa(E) = A' \frac{(E - E_g)^2}{E^2 - BE + C} \quad (10)$$

where  $A'$  is proportional to the matrix element of the dipolar transition,  $B = 2(E_f - E_i)$  and  $C = (E_f - E_i)^2 - \hbar^2/4\tau^2$ . Subscripts  $i$  and  $f$  refer to initial and final state respectively. Hence  $(E_f - E_i) = B/2$  corresponds to the peak transition energy (as in the case of  $E_0$  in the TL model). Contrasting with Tauc-Lorentz model, FB ones considers that the square of the dipolar matrix element is a constant. In the case of dispersed carbon in our composite film, the validity of the model is checked by introducing a figure-of-merit based on equalities of peak transition and maximum absorption energies derived from the models.  $\varepsilon_2(E)$  and  $\kappa(E)$  were fitted to TL and FB models through numerical simulations and are shown in Fig.5 (a) and (b) respectively.

From the fit parameters, we derived the transition lifetime  $\tau$  and the peak transition energy ( $B/2$  for FB fit,  $E_0$  for TL fit). All these values are summarised in Table 1.

### 3.5- Modification of FB model:

Results of TL and FB models given above yield lifetimes of the same order, though giving different energy gap values. Both models use different assumptions about the energy dependence of the matrix element of the transition (momentum versus dipole taken as a constant matrix element); as a consequence, this may explain the great difference between  $E_0$  given by TL and  $B/2$  given by FB. Furthermore, the values within both models are unrealistic, too high for TL and too low for FB. The optical properties of the amorphous C films are known to be dominated by the  $\pi$ - $\pi^*$  and  $\sigma$ - $\sigma^*$  electron transitions, along with the  $\pi$ - $\sigma^*$  and  $\sigma$ - $\pi^*$  transitions [23, 24]. The  $\pi$ - $\pi^*$  contribution originates exclusively from  $sp^2$  carbon. The  $\sigma$ - $\sigma^*$  transitions occurs at  $\sim 14$  eV in graphite and at  $\sim 11$  eV in diamond, while the  $\pi$ - $\pi^*$  transition is located at  $\sim 4$  eV. All these values of energy correspond to the maximum absorption for a specific interband transition. Consequently, no transition other than the  $\pi$ - $\pi^*$  can contribute to optical absorption in the visible range.

Further, the self-consistency of the simulation data for a given model should be checked within the frame of its own formulation. If  $E_{\max}$  is the energy of maximum absorption (maximum  $\kappa$  for FB and maximum  $\varepsilon_2$  for TL) according to the model formulation, it should be very close to  $E_0$  for TL and  $B/2$  for FB as they have the same physical significance. It is clear from Table 1 that this self-consistency is not verified for any model when applied to the present films. The discrepancy between the two parameters from FB formulation is the largest. In order to make FB model applicable to our films, an energy dependence in the squared matrix element  $R^2(E)$  of the transition dipole has been introduced in it. This energy dependence  $R^2(E) \propto E^{-2}$  is then introduced in  $\kappa(E)$  as follows:

$$\kappa(E) = \frac{1}{E^2} \frac{A^* (E - E_g)^2}{E^2 - BE + C} \quad (11)$$

Our choice of this dependence of  $R^2(E)$  is based on earlier indications of a  $E^{-2}$  energy scaling of matrix elements in disordered materials [25].

The best fit of  $\kappa(E)$  with this formulation is shown in Fig. 5 (c), fit values being given in Table 1. The figure-of-merit  $B/2 = E_{\max}$  is now fairly achieved. Furthermore, the energy gap  $E_g$  from our modified FB model (designed as mFB in Table 1) and from TL are much closer than in the case of

the original FB. However, the modified FB model appears superior to TL in that it gives a much more realistic peak transition energy (4.23 versus 11.04 eV).

#### 4- Conclusion

Fitting the experimental reflectance spectra to a Maxwell-Garnett effective medium theory leads to the optical constants of each component of the composite film as well as its effective dielectric constants. The parameters of absorption of the carbon phase i.e. band gap energy, peak transition energy and lifetime of optical transition could thus be determined using Tauc-Lorentz (TL) and Forouhi-Bloomer (FB) models. The latter have been applied to the optical constants, with the introduction of a figure-of-merit based on equalities of peak transition and maximum absorption energies derived from the models. The results show the adequacy of FB model to describe the interband transitions of the amorphous carbon phase of the composite films, provided an energy dependence of the dipole matrix element of the transition is introduced. Band-gap energy and electron transitions in the transparent zirconia phase of the films were determined by examining the energy loss features along the excitation of O1s and Zr3d core levels..

#### Acknowledgments

This work was supported by Autonomous Province of Trento (Fondo Progetti Ricerca) under MicroCombi project.

#### References

- [1] M. Hirano, S. Watanabe, E. Kato, Y. Mizutami, M. Kawai, Y. Nakamura, *Solid State Ionics* 111 (1998) 161
- [2] M. Zevin, R. Reisfeld, *Opt. Mater.* 8 (1997) 37
- [3] X. Guo, R. Waser, *Progr. Mater. Sci.* 51 (2006) 151
- [4] I. Balberg, *Carbon* 40 (2002) 139
- [5] D. Fink, R. Klett, L. T. Chadderton, J. Cardoso, R. Montiel, H. Vazquez, A. A. Karanovich, *Nucl. Instr. Meth. B* 111 (1996) 303
- [6] R. Dominko, M. Gaberscek, J. Drogenik, M. Bele, J. Jamnik, *Electrochim. Acta*, 48 (2003) 3709
- [7] S.-L. Shi, J. Liang, *J. Appl. Phys.* 101 (2) (2007) 023708
- [8] G. E. Jellison, Jr and F. A. Modine, *Appl. Phys. Lett.* 69 (3) (1996) 371
- [9] A. R. Forouhi and I. Bloomer, *Phys. Rev. B* 34 (10) (1986) 7018
- [10] N. Laidani, V. Micheli, M. Anderle, *Thin Solid Films* 382 (2001) 23
- [11] H. Holleck, *J. Vac. Sci. Technol. A*, 4 (6) (1986) 2661
- [12] L. Calliari, M. Filippi, N. Laidani, M. Anderle, *J. Electron Spectrosc.* 150 (2006) 40
- [13] G. R. Corallo, D. A. Asbury, R. E. Gilbert, G. B. Hoflund, *Phys. Rev. B* 35 (18) (1987) 9451
- [14] F. Yubero, J. P. Espinòs, A. R. González-Elipe, *J. Vac. Sci. Technol. A* 16 (4) (1998) 2287
- [15] D. W. McComb, *Phys. Rev. B* 54 (10) (1996) 7094
- [16] R. H. French, S. J. Glass, F. S. Ohuchi, Y.-N Xu, W. Y. Ching, *Phys. Rev. B* 49 (8) (1994) 5133
- [17] H. Nohira, W. Tsai, W. Besling, E. Young, J. Petry, T. Coanrd, W. Vandervorst, S. De Gendt, M. Heyns, J. Maes, M. Tuominen, *J. Non-Cryst. Solids* 303 (2002) 83
- [18] Y. Wang, Y. Abe, Y. Matsuura, M. Miyagi, and H. Uyama, *Appl. Opt.* 37 (1998) 7091
- [19] M. Born, E. Wolf, " *Principles of Optics*", ( 7<sup>th</sup> ed., Cambridge University Press, Cambridge, MA, 1999)
- [20] P. Cheyssac, *Opt. Commun.* 268 (2006) 273
- [21] J. C. Maxwell-Garnett, *Phil. Trans. Roy. Soc.* 205 (1906) 237; J. C. Maxwell-Garnett, *Phil. Trans. Roy. Soc.* 203 (1904) 385
- [22] G. Ghosh , "Handbook of thermo-optics coefficients of optical materials with applications."

(Academic Press, 1998) pp. 5-110

[23] J. Daniels, C. V. Festenberg, H. Raether and K. Zeppenfeld, "Optical Constants of Solids by Electron Spectroscopy", Springer Tracts in Modern Physics, Vol. 54 (G. Hohler, ed., Springer-Verlag Berlin, 1970), pp. 77-135

[24] S. Logothetidis, *Diam. Relat. Mater.* 12 (2003) 141

[25] G. A. N. Connel, "Optical properties in amorphous semiconductors", Springer Topics in Applied Physics, *Amorphous Semiconductors*, vol 36 (Ed. M. H. Brodsky, Berlin: Springer, 1979) pp 73-111.

Table 1: Fit parameters of Tauc-Lorentz (TL) and both un-modified (FB) and modified Forouhi and Bloomer (m-FB) models for, respectively,  $\varepsilon_2(E)$  and  $\kappa(E)$  constants of the C phase of the films.

<b>TL model</b>		<b>FB model</b>		<b>m-FB</b>	
A (eV)	48.127	A'	0.452	A* (eV <sup>2</sup> )	3.525
E <sub>0</sub> (eV)	11.039	B/2 (eV)	1.412	B/2 (eV)	4.23
Γ (eV)	13.99	C (eV <sup>2</sup> )	16.751	C (eV <sup>2</sup> )	25.479
E <sub>g</sub> (eV)	0.771	E <sub>g</sub> (eV)	0.252	E <sub>g</sub> (eV)	0.862
τ (s)	4.71 x 10 <sup>-17</sup>	τ (s)	8.90 x 10 <sup>-17</sup>	τ (s)	1.95 x 10 <sup>-16</sup>
E <sub>max</sub> (eV)	9.21	E <sub>max</sub> (eV)	14.14	E <sub>max</sub> (eV)	4.59
χ <sup>2</sup>	1.6537 x 10 <sup>-7</sup>	χ <sup>2</sup>	2.5971 x 10 <sup>-8</sup>	χ <sup>2</sup>	1.2105 x 10 <sup>-8</sup>
R <sup>2</sup>	1	R <sup>2</sup>	0.99998	R <sup>2</sup>	0.99999

## Figure captions

Figure 1: XPS spectra of

- (a) valence band
- (b) loss spectrum associated with Zr3d core level spectrum, with curve fitting.

Figure 2: Basic principle of band-gap determination shown on (a) O1s and (b) Zr3d XP spectra and their derivatives. This energy corresponds to the onset of the electron transition excitations, evidenced on the derivative spectra.

Figure 3: (a) Schematic multilayered structure of the film / PC system (numbers indicate the  $i$ -th layers).  
(b) measured reflectance of a bare PC (curve 1, continuous line) and of  $\text{ZrO}_{2-x}$ -C film on PC (curve 2), calculated reflectance of PC (curve 3, full symbols) and of  $\text{ZrO}_{2-x}$ -C film on PC (curve 4).

Figure 4: (a) Real part of dielectric constant of the carbon phase  $\epsilon_1$ , the matrix  $\epsilon_{m1}$  and the composite  $\langle \epsilon \rangle_1$  and imaginary part of dielectric constant of the composite  $\langle \epsilon \rangle_2$ ,  
(b) Real part of the index of the carbon phase,  $v$ , and the matrix,  $v_m$  and imaginary part  $\kappa$  of the index of the carbon phase, versus photon energy  $E$  for  $\text{ZrO}_{2-x}$ -C film.

Figure 5: (a)  $\epsilon_2(E)$  fitted to TL model  
(b)  $\kappa(E)$  fitted to FB model  
(c)  $\kappa(E)$  fitted to modified FB model for the C phase of the film.

Figure 1

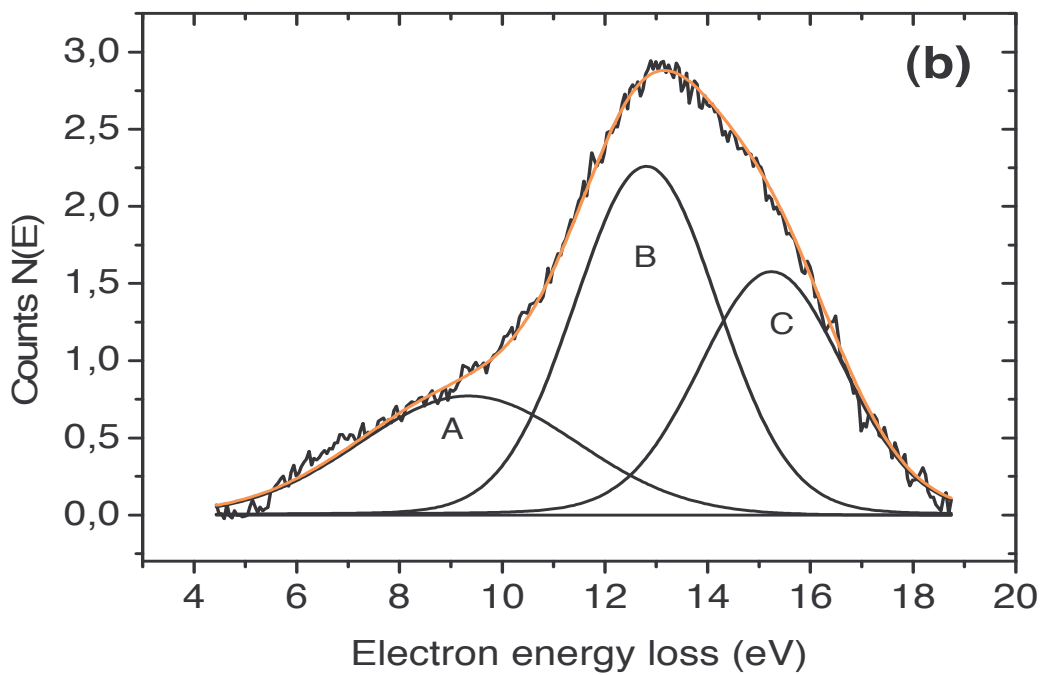
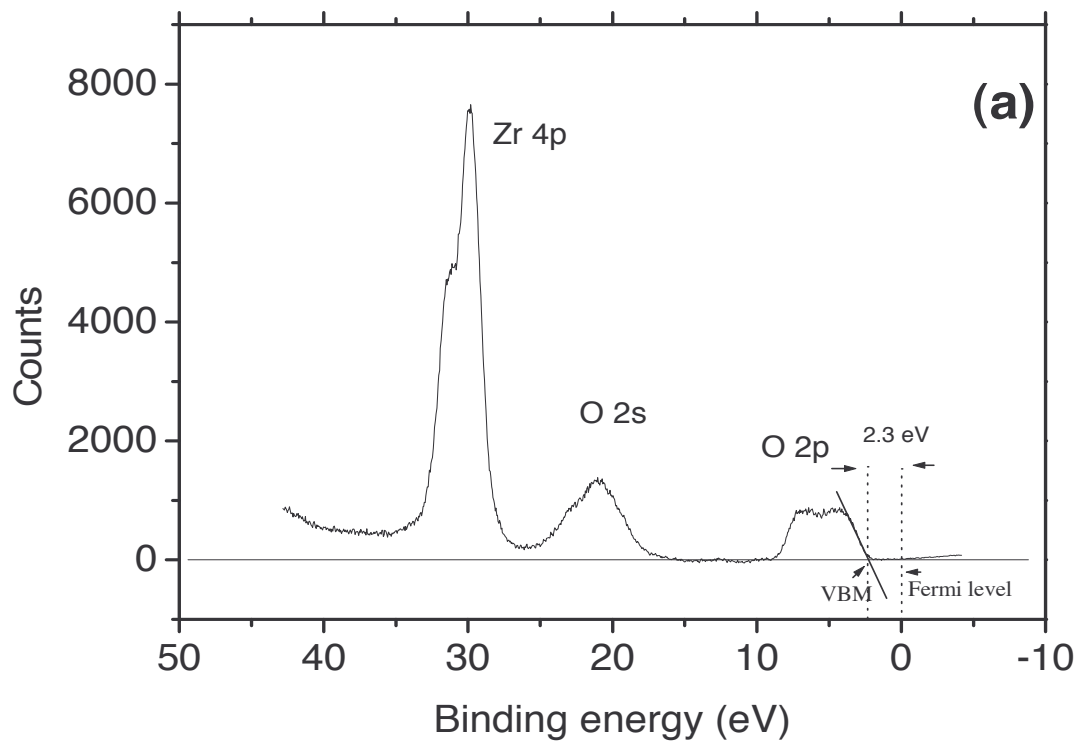


Figure 2

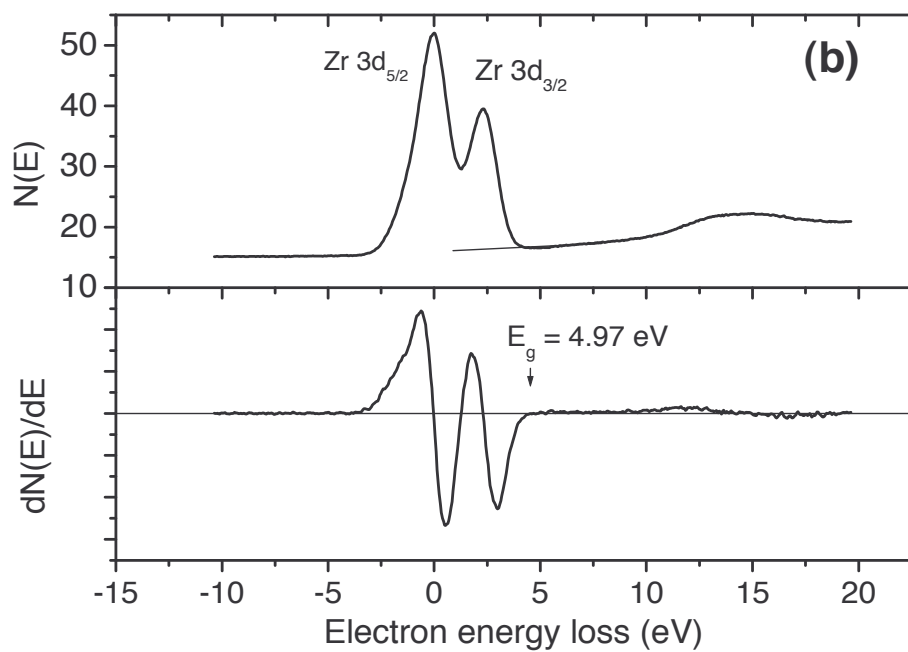
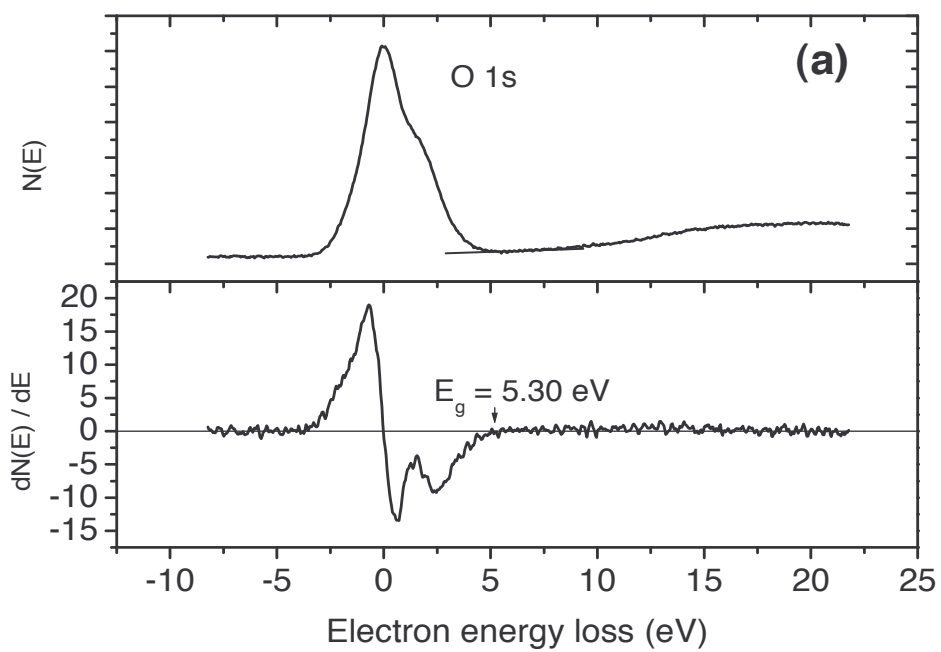


Figure 3

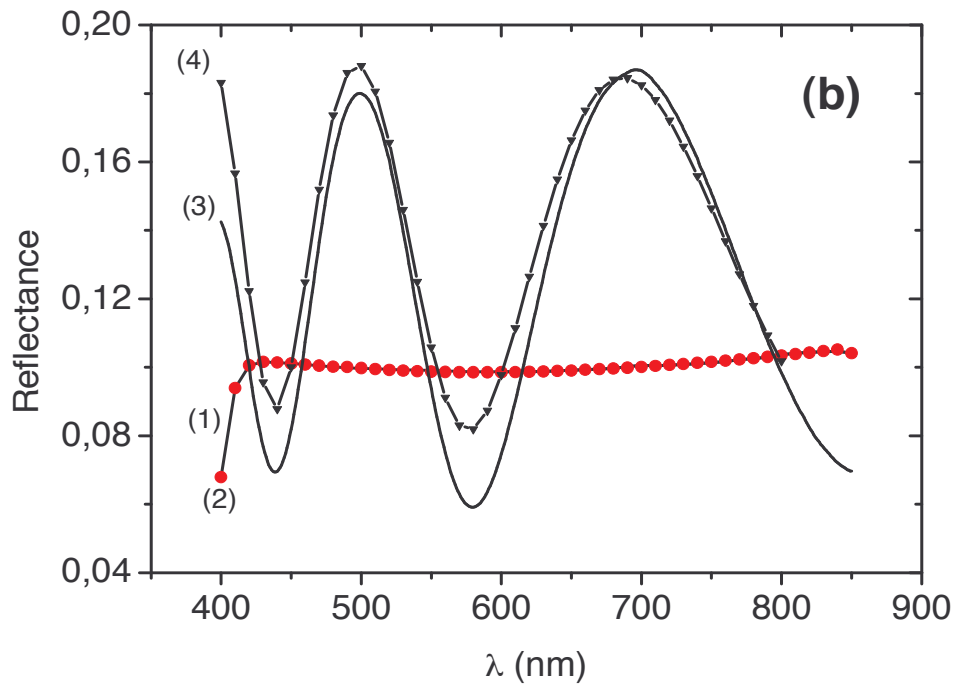
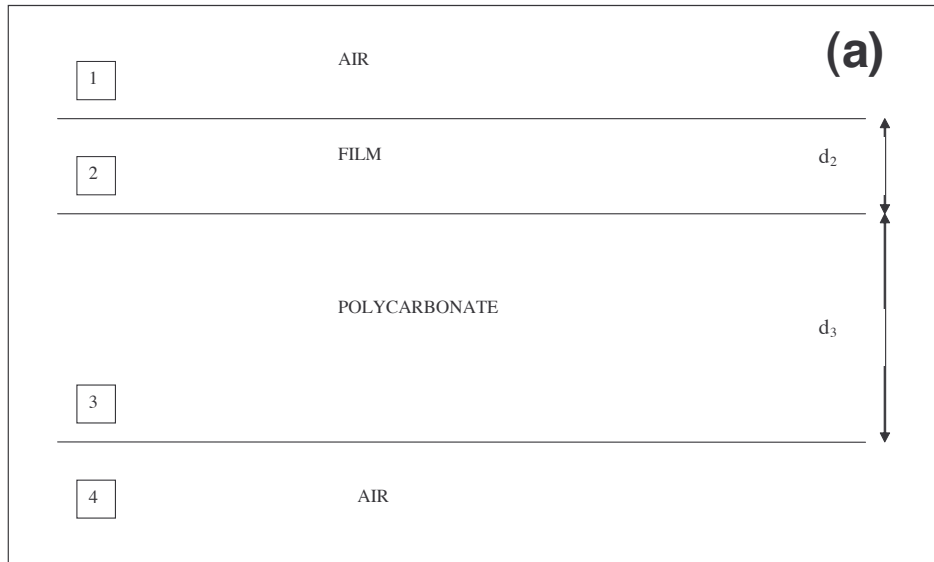


Figure 4

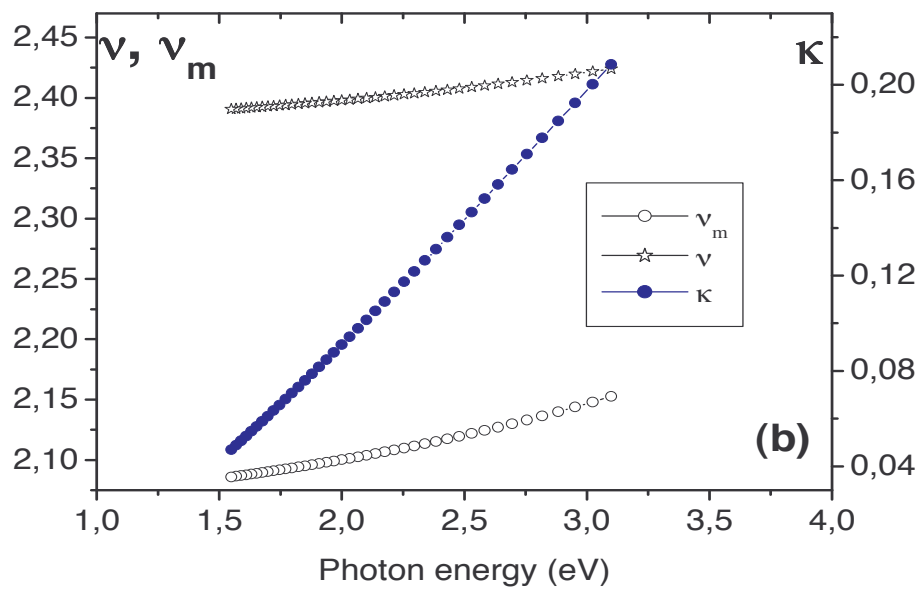
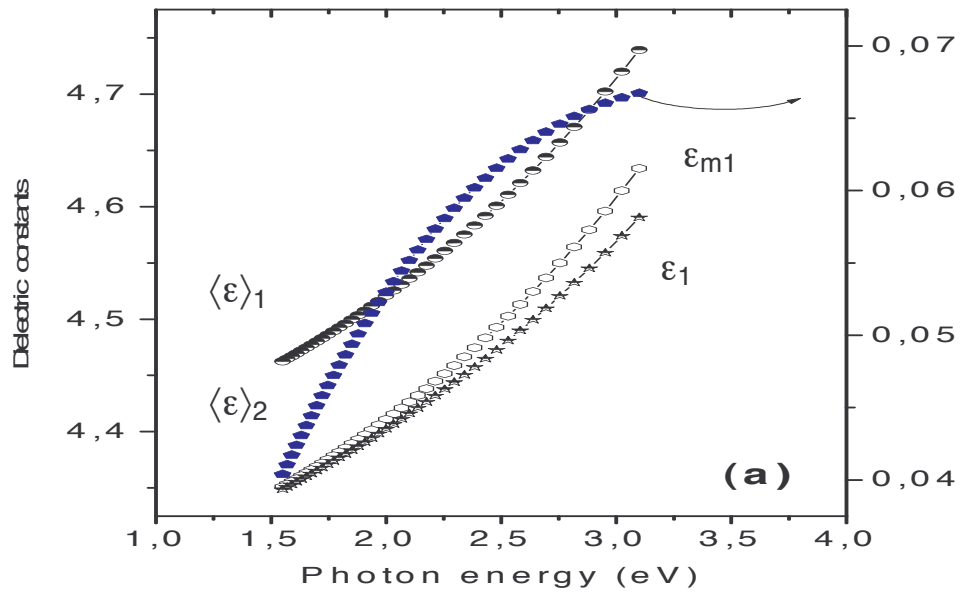


Figure 5

